ELSEVIER

Journal of Magnetism and Magnetic Materials 238 (2002) 246–251

Journal of magnetism and magnetic materials

www.elsevier.com/locate/jmmm

Micromagnetic simulations of the domain structure and the magnetization reversal of $Co_{50}Ni_{50}$/Pt multilayer dots

S. Sindhu, M.A.M. Haast, K. Ramstöck, L. Abelmann, J.C. Lodder*

Information Storage Technology Group, MESA Research Institute, University of Twente, P.O. Box 217, 7500 AE, Enschede, The Netherlands

Received 15 November 2000

Abstract

The domain structure and the switching field of $Co_{50}Ni_{50}$/Pt multilayer dots, prepared by laser interference lithography, were micromagnetically simulated. The simulations were carried out with a three-dimensional simulation package, optimized for large-scale problems. The single-domain state is the lowest energy state for dots with a diameter below 75 nm. The switching field was computed by using suitable minimization techniques, and was used to analyze the effect of size, dot shape and edge defects.

PACS: 75.60; 75.40.Mg

Keywords: Numerical micromagnetics; Domain observation; Magnetic dots; Magnetization reversal; Hysteresis; Patterned media

1. Introduction

Micromagnetism plays an important role in designing magnetic storage devices with improved characteristics and has become an area of scientific and technological interest [1–9]. Micromagnetics, though more demanding than finite element methods that neglect exchange energy or analytical techniques, gives more reliable results on small structures and allows us to model the influence of a larger number of parameters.

Magnetic imaging and micromagnetic simulations have shown that non-uniform magnetization configurations in patterned structures can considerably affect the magnetization reversal [10,11]. The mode of reversal directly determines the energy barrier that has to be overcome for switching. If patterned elements are going to be used for data storage, in the so-called *patterned media*, this barrier should be as high as possible, so that very small magnetic elements will still be thermally stable. Moreover, domain walls and ripple structures, which contribute to noise in the read-back signal, limit the storage density in these patterned media and should, therefore, be carefully analyzed [12].

The ultimate storage density in patterned media can be achieved if a regular matrix of single-domain dots with a uniaxial anisotropy is used [13,14], and each dot represents exactly one bit in its up or down state. The superparamagnetic bit density limit of this type of medium is much higher

*Corresponding author. Tel.: +31-53-489-2750; fax: +31-53-489-3343.

E-mail address: j.c.lodder@el.utwente.nl (J.C. Lodder).

0304-8853/02/$ - see front matter
PII: S0304-8853(01)00919-2

than that of the thin continuous film media, where hundreds of uncoupled grains are needed to store one bit of information [15].

Detailed understanding of the domain structure and the magnetization reversal in such patterned media is important. As the shape is strongly non-ellipsoidal, a Stoner–Wohlfarth model [16] would be a very rough guess only. In this paper, we, therefore, use an existing micromagnetic simulation package [17] to investigate the domain structure and magnetization reversal of small circular elements, which is not only of importance for patterned media, but also for non-volatile magnetic memories [18].

2. Experimental details

The elements treated in this paper are (Pt(6Å)/$Co_{50}Ni_{50}$(6Å)/Pt(6Å))$_{26}$ multilayer dots with large intrinsic perpendicular magnetic anisotropy and strong intergranular exchange coupling, prepared by magnetron sputtering. The patterned array is realized by Laser Interference Lithography and ion beam etching [19,20]. A SEM picture of the dots, including the remains of the photoresist, is shown in Fig. 1. In this sample, the distance between the dots is 200 nm and the dot sizes varied from 60 to 80 nm.

The equilibrium domain configuration in these dots changes with dot diameter. Fig. 2 shows, for instance, the MFM images of the domain state after in-plane demagnetization of samples with a dot diameter of 180 nm, revealing a multidomain structure with two or three domains per dot (a), and dots with a diameter of 70 nm, which are all in a single-domain (SD) state (b). These dots are not perfect cylinders due to etching damage, but appear as truncated cones.

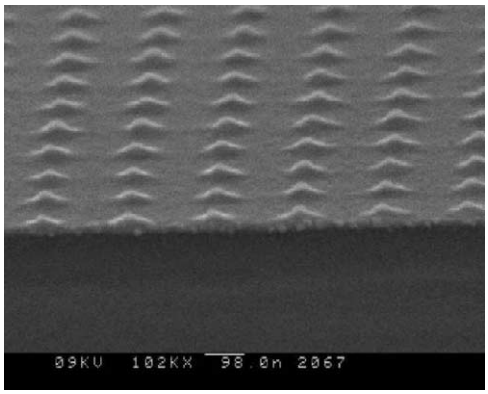

Fig. 1. SEM image of 60–80 nm sized $Co_{50}Ni_{50}$/Pt multilayer dots.

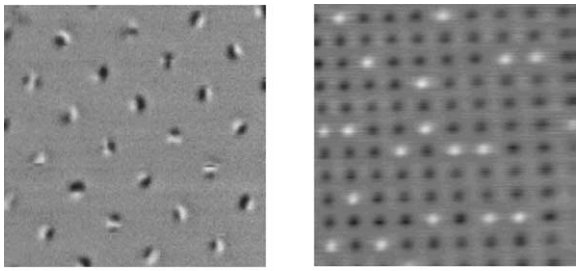

Fig. 2. (a) MFM images of 180, and (b) 70 nm $Co_{50}Ni_{50}$/Pt multilayer dots.

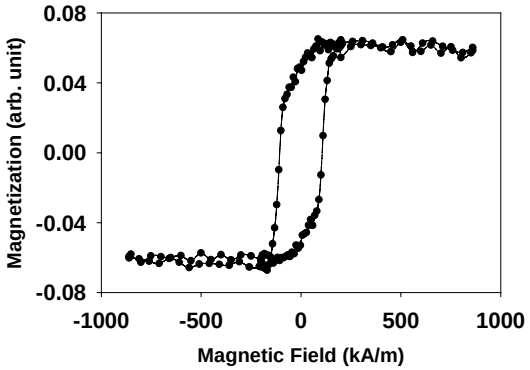

Fig. 3. VSM hysteresis curve of 70 nm $Co_{50}Ni_{50}$/Pt multilayer dots.

Fig. 3 shows the hysteresis loop obtained from a vibrating sample magnetometer for an area of $1 \times 1\,cm^2$ patterned $Co_{50}Ni_{50}$/Pt multilayer dots of 70 nm size. The experimental results show that the switching field, H_{sw}, is approximately 120 kA/m ($H_{sw}/H_k = 0.08$). The magnetization reversal does not show a sharp switching behavior. This is believed to be due to the inhomogeneity in the dot size and shape that would cause a widened switching distribution. For the simulations, however, the dots are modeled to be homogeneous in size, the parameters being listed in Table 1.

Table 1
Homogeneous dot parameters used for simulation

Parameter	Value (SI)	Value (CGS)
Uniaxial anisotropy constant K_u	$480\,kJ/m^3$	4.8×10^6 erg/cc
Exchange constant A	3×10^{-12} J/m	3×10^{-7} erg/cm
Saturation magnetization M_s	713 kA/m	713 emu/cc
Anisotropy field H_k	1500 kA/m	18.8 kOe

3. Micromagnetic simulations

The domain structure and magnetization reversal mechanism of one single $Co_{50}Ni_{50}$/Pt multilayer dot is carried out with a 3D-micromagnetic-simulation package. The algorithm used [17] is a straightforward extension of the one described in [21,22] to three dimensions. Due the constraints imposed by the FFT method used for stray field computation, a uniform grid and rectangular computational area are needed. Arbitrary shapes are handled by setting the magnetization outside the sample to zero. Special precautions are taken at the outer, curved, surfaces. The volume fraction of cells that lie partly outside the sample is taken into consideration and surface changes are carefully calculated using the surface normal of the intended, cylindrical, shape.

The energy terms considered are the exchange coupling (E_x), uniaxial anisotropy (E_k), stray field (or demagnetization) (E_d) and external field (E_z) contributions.

$$E_{tot} = E_x + E_k + E_d + E_z[J]. \quad (1)$$

This total energy is minimized using minimization techniques called modified steepest descent and relaxation (MSDR) [23,24] to find the non-uniform magnetization and wall geometry. We find this method to be faster than conjugate gradients and relaxation via the Landau–Lifshitz Gilbert (LLG) equation [25,26]. This approach also allows to easily select different states, by using suitable starting configurations; whereas the transition between these states cannot be modeled directly, the limit of stability of these states can be found and the point of equal energy can be determined. This defines a regime around which specimens should change behavior.

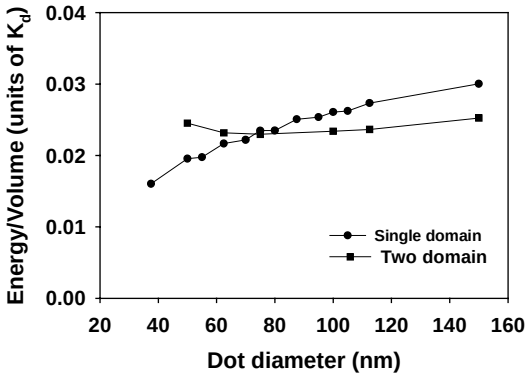

Fig. 4. Critical size of CoNi/Pt multilayer dots with $h = 30$ nm.

To eliminate the effect of discretisation, the total energy simulated is plotted against 1/(number of cells) and is extrapolated to obtain an estimate of the energy at an infinite number of cells. The experimental parameters given in Section 2 are used as the input parameters. Like indicated before, we modeled the CoNi/Pt multilayer dots by a homogeneous material with a saturation magnetization smaller than CoNi.

The critical size at which the energy of SD state equals that of the two-domain (TD) state, as well as the switching field distribution of such SD dots are studied. By investigating stable configurations from different initial configurations and comparing the energies as a function of cell size, a set of equilibrium states are found. Using this procedure, the energy of dots of height 30 nm in SD and TD states are calculated as a function of dot diameter.

Fig. 4 shows the calculated total minimum energy density as a function of dot diameter for the SD and TD states. The energy is calculated using the following procedure. First, the domain

configuration is initialized in a SD state. After relaxation, this state remains stable for a certain range of dot diameters, and the total energy of the SD configuration can be calculated as a function of dot diameter. In the SD state, there is no domain wall so the exchange and anisotropy energy are negligible. Therefore, the demagnetization energy is the dominant energy contribution and it makes sense to divide the total energy density e_{tot} by the maximum demagnetisation energy density $k_d = 1/2\mu_0 M_s^2/V$. Recognizing that e_d/k_d is for the SD state approximately equal to the demagnetization factor along the axis of a cylinder, it can be understood that $e_d \approx e_{tot}$ increases with increasing cylinder diameter.

Next, the domain configuration is initialized in a TD configuration and using the same procedure the energy is plotted against the dot size. The demagnetization energy of the TD state strongly reduces with respect to the SD and becomes comparable to the exchange and anisotropy energy. The exchange and anisotropy energy originate mainly from the domain wall and scale linearly with dot diameter. After dividing by the dot volume, which scales with the diameter squared, the relative contribution of exchange and anisotropy energy, or "wall-energy", *decreases* with increasing dot diameter. This effect is counterbalanced by the fact that the demagnetization energy density *increases* with increasing dot diameter, as in the case of SD. Of course, at a certain dot diameter the creation of yet another domain becomes favorable and a three-domain state is formed, as can be seen in Fig. 2.

The energy density plots of the SD and TD states intersect at about 75 nm, which is defined as the critical diameter. The SD state is the lowest energy state in dots with diameters below the critical diameter. Above this diameter, it is energetically more favorable for the dot to split into two domains because this decreases the total energy. Indeed, experiments showed that 70 nm dots, which are just below the critical diameter, were never observed in the TD state, whereas after

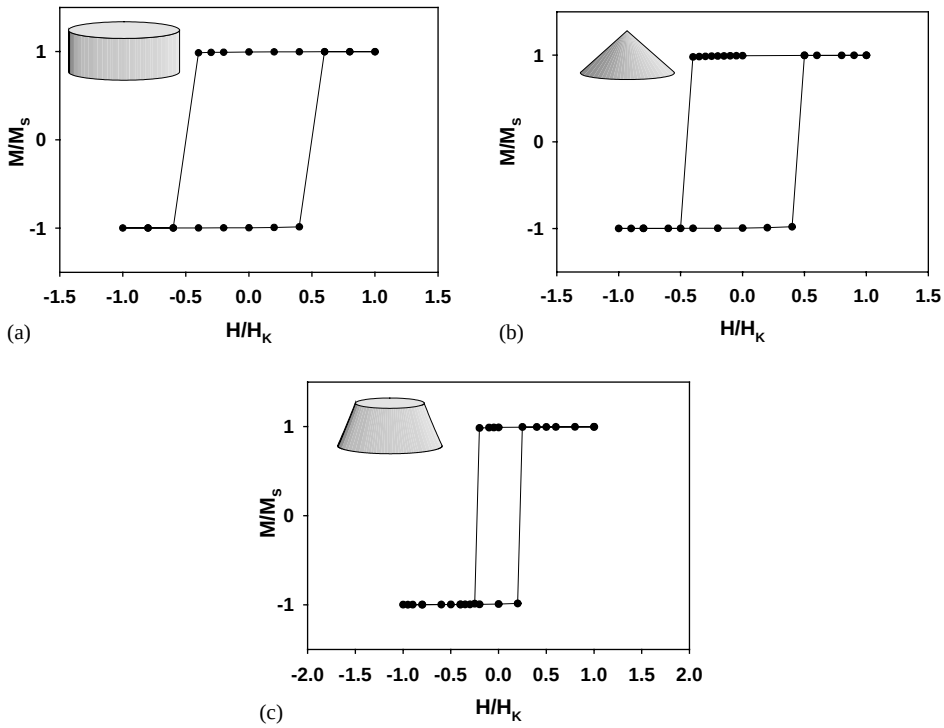

Fig. 5. Magnetization reversal of CoNi/Pt multilayer dots with (a) cylindrical, (b) pointed cone, and (c) truncated cone shape.

proper demagnetisation, 180 nm dots are multi-domain (see Fig. 2).

The magnetization as a function of external field is simulated in order to obtain the switching field (H_{sw}) of a cylindrically shaped $Co_{50}Ni_{50}$/Pt dot with a diameter of 70 nm and height of 30 nm. Fig. 5(a) shows the magnetization reversal and H_{sw}/H_k can be estimate to be 0.50 (where H_k, the anisotropy field, is 1500 kA/m), which is much higher than the measured value of 0.08. It is known that the exact shape of small magnetic elements strongly influences the switching field [27]. Therefore, the slanting of the side walls of the dots, resulting from the imperfect resist pattern shape, was included. Initially, the dots were modeled as *pointed* cones, which resulted in a slightly lower H_{sw}/H_k value of 0.43 (Fig. 5a). The simulation was repeated with *truncated* cones, i.e. taking the bottom diameter and the top diameter in the ratio 1:2 and 1:1.5 (Fig. 5b). Even lower H_{sw}/H_k values of, respectively, 0.375 and 0.22 for these shapes were found, but still much higher than the measurement.

Etch damage and imperfect layer growth might also influence the switching field. Therefore, the simulation was repeated for a truncated cone shape with ratio 1:1.5 (Fig. 5c) with an outer soft shell in the circumference of the dot. (The top layer is protected by resist.) This shell has an anisotropy value reduced to 15% of the bulk value. Another soft layer was implemented at the bottom of the dot to account for the fact that the initial growth of the multilayer stack is poor, which reduces the anisotropy in the first few bilayers. The thickness of the soft layer in the circumference as well as in the bottom layer is 10 nm, see Fig. 6. The simulated hysteresis curve of this geometry

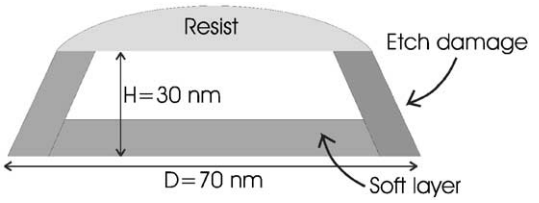

Fig. 6. Sketch of CoNi/Pt multilayer dot showing the location of the residual resist layer, the etch damage layers around the dot and the soft initial layer in the bottom.

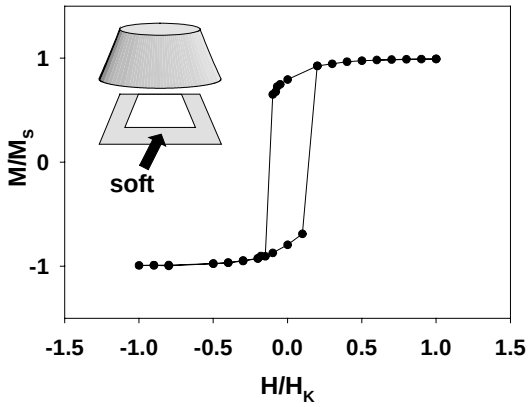

Fig. 7. Magnetization reversal of CoNi/Pt multilayer truncated cone shaped dot with additional soft layers (see Fig. 7).

(Fig. 7) shows that the addition of the soft layers reduces the value of H_{sw}/H_k further down to 0.13, now approaching the measured value.

4. Conclusion

Large-scale 3D micromagnetic simulations predict that in 30 nm thick CoNi/Pt multilayered dots with properties, as in Table 1, the single-domain state is the lowest energy state for dot diameters below 75 nm. This is in agreement with experiments that show that the two-domain state is stable in 180 nm dots but not in 70 nm dots.

The agreement between the simulated and measured switching is not very good if perfect cylindrical dots are assumed: the simulated switching fields are much higher. The simulations shows that imperfections such as deviations from the cylindrical shape and local anisotropy variations have a significant effect on the switching field, as well as the presence of softer layers, caused by, for instance, etch damage or bad initial growth of the multilayer structure. If in the simulation, a more realistic shape of a truncated cone is combined with a soft outer shell and bottom layer, a switching field of 0.13 H_k is obtained, which is getting close to the measured value of 0.08. The simulations, therefore, indicates that a development of an optimized patterning process, which

reduces the etching damage and slanted side wall, may considerably enhance the switching field. This is an important conclusion for the application of this type of dots in storage systems.

Another reason for the high value of the simulated switching fields could be that computer resources prevent us to simulate the layered structure of the dots—instead a uniform material with averaged properties was assumed. One can imagine that switching is nucleated in one of the individual CoNi layers, which will surely decrease the switching field. Next to this, the effect of temperature and the true precession of the spins are not included in the simulation, again because of computer resources. With increasing memory size and processor speed and decreasing dot size, future simulation might include these properties, and better agreement between simulated and measured switching fields could be obtained.

Acknowledgements

The authors are thankful to the Dutch Foundation for Fundamental Research on Matter (FOM) and Dutch Technology Foundation (STW) for financial assistance. The research of Leon Abelmann has been made possible by a fellowship of the Royal Netherlands Academy of Arts and Sciences (KNAW).

References

[1] J.F. Smyth, S. Schultz, D.P. Kern, H. Schmid, D. Yee, J. Appl. Phys. 63 (1988) 4237.
[2] R.M.H. New, R.F.W. Pease, R.L. White, R.M. Osgood, K. Babcock, IEEE Trans. Magn. 31 (1995) 3601.
[3] T. Zhu, J. Shi, K. Nordquist, S. Tehrani, M. Durlam, E. Chen, H. Goronkin, IEEE Trans. Magn. 33 (1995) 3601.
[4] Y.F. Zheng, J.-G. Zhu, IEEE Trans. Magn. 32 (1996) 4237.
[5] S.T. Chui, V.N. Ryzhov, Phys. Rev. Lett. 78 (1997) 2224.
[6] S.T. Chou, P.R. Krauss, L. Kong, J. Appl. Phys. 79 (1996) 6101.
[7] M. Lederman, G.A. Gibson, S. Schultz, J. Appl. Phys. 73 (1993) 6961.
[8] E. Gu, E. Ahmad, S.J. Gray, C. Daboo, J.A.C. Bland, L.M. Brown, M. Ruhrig, A.J. Mc Gibbon, J.N. Chapman, Phys. Rev. Lett. 78 (1987) 1158.
[9] K.J. Kirk, J.N. Chapman, C.D.W. Wilkinson, Appl. Phys. Lett. 71 (1997) 539.
[10] Y.F. Zheng, J.-G. Zhu, J. Appl. Phys. 81 (1997) 5471.
[11] J. Shi, T. Zhu, M. Durlam, E. Chen, S. Tehrani, Y.F. Zheng, J.-G. Zhu, IEEE Trans. Magn. 34 (1998) 997.
[12] A.M. Barany, H.N. Bertram, IEEE Trans. Magn. 23 (1987) 1776.
[13] D.E. Speliotis, J. Magn. Magn. Mater. 193 (1999) 29.
[14] S.Y. Chou, Proc. IEEE 85 (1997) 652.
[15] R.L. White, J. Magn. Magn. Mater. 209 (2000) 1.
[16] E.C. Stoner, E.P. Wohlfarth, IEEE Trans. Magn. 27(4) (1991) 3475–3518 (reprinted from Trans. R. Soc. London Ser. A. 240 (1948) 599–642).
[17] K. Ramstöck, J.J.M. Ruigrok, J.C. Lodder, Sensors Actuators A 81 (1–3) (2000) 359–362. Also see http://www.ramstock.de.
[18] M. Johnson, J. Vac. Sci. Technol. A16 (1998) 1806; G.A. Prinz, Science 282 (1998) 1660.
[19] M.A.M. Haast, I.R. Heskamp, L. Abelmann, J.C. Lodder, Th.J.A. Popma, J. Magn. Magn. Mater. 193 (1999) 511.
[20] M.A.M. Haast, J.R. Schuurhuis, L. Abelmann, J.C. Lodder, Th.J.A. Popma, IEEE Trans. Magn. 34 (1998) 1006.
[21] D.V. Berkov, K. Ramstöck, A. Hubert, Phys. Stat. Sol. (a) 137 (1993) 207.
[22] A. Hubert, R. Schäfer, Magnetic Domains: The Analysis of Magnetic Microstructures, Springer, Berlin, Heidelberg, New York, 1998, p. 396.
[23] D.V. Berkov, K. Ramstöck, T. Leibl, A. Hubert, IEEE Trans. Magn. 29 (1993) 2548.
[24] M.E. Schabes, A. Aharoni, IEEE Trans. Magn. 23 (1987) 3882.
[25] L.D. Landau, E. Lifshitz, Phys. Z. Sowjetunion. 8 (1935) 153.
[26] T.L. Gilbert, Phys. Rev. 100 (1955) 1243.
[27] R. Mattheis, K. Ramstöck, J. McCord, IEEE Trans. Magn. 33 (5) (1997) 3993.